Swiss Federal Institute of Technology Zurich

PAUL SCHERRER INSTITUT

Weizmann Institute of Science

Rehovot, 26.11.2012

Solar thermochemical

H_2O and CO_2 splitting

utilizing a reticulated porous ceria redox system

Philipp Furler

Daniel Marxer

Jonathan Scheffe

Aldo Steinfeld

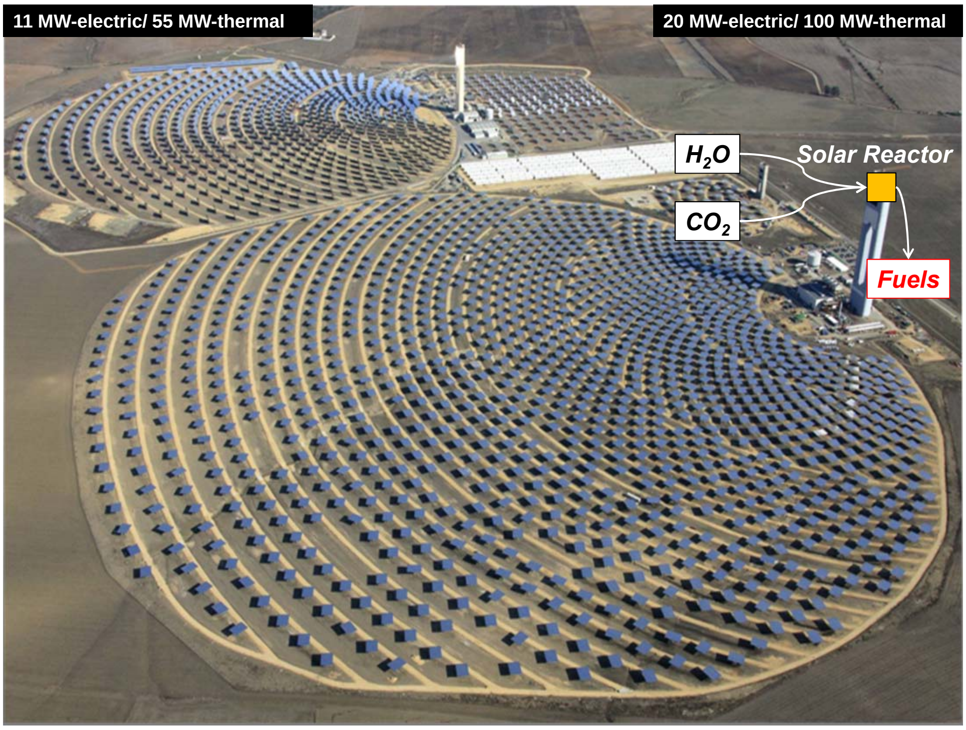

Thermolysis

$$H_2O \rightarrow H_2 + \tfrac{1}{2} O_2$$
$$CO_2 \rightarrow CO + \tfrac{1}{2} O_2$$

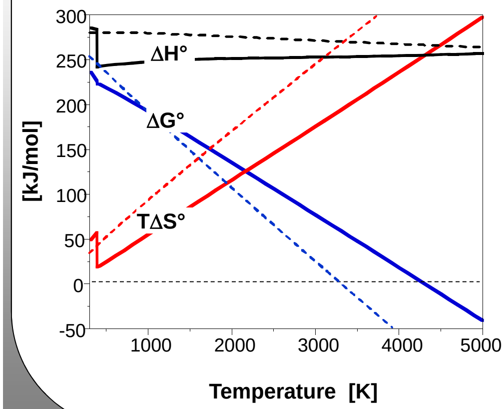

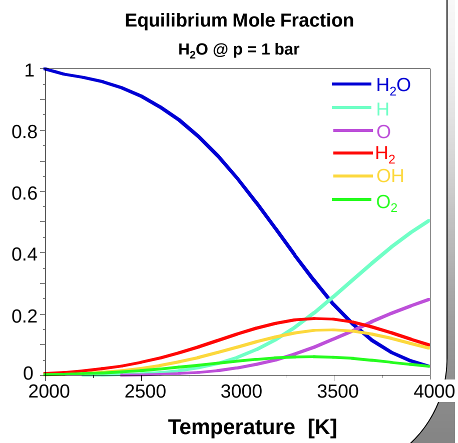

Solar Thermochemical Splitting of H_2O and CO_2

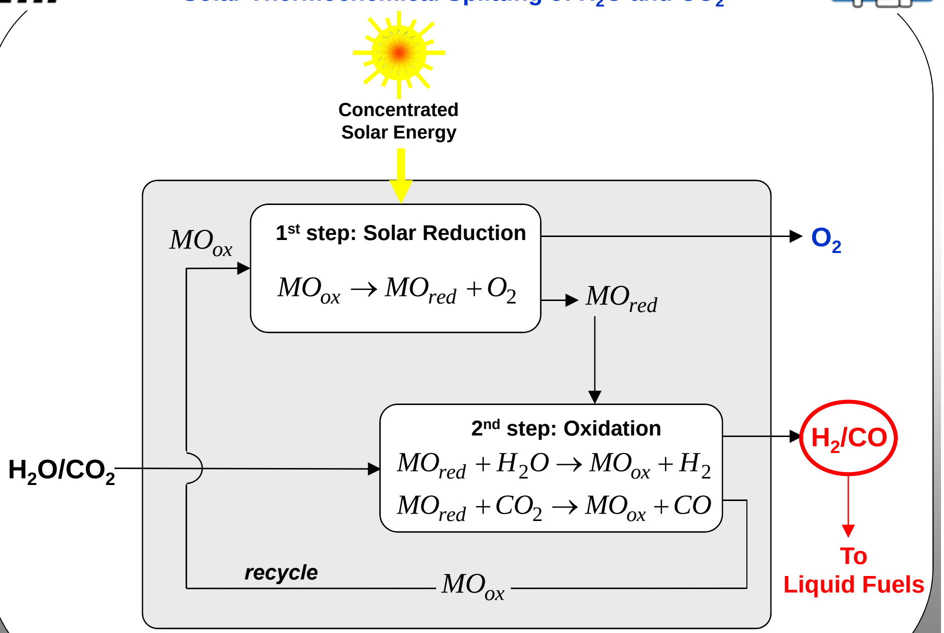

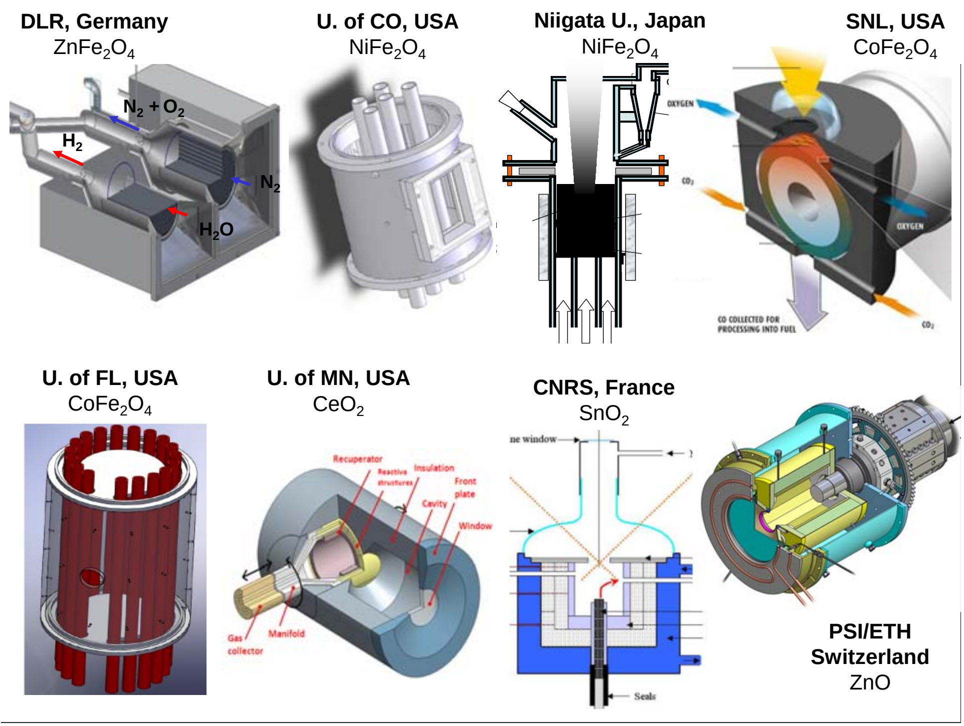
DLR, Germany
$ZnFe_2O_4$
$N_2 + O_2$
H_2
N_2
H_2O
U. of CO, USA
$NiFe_2O_4$
Niigata U., Japan
$NiFe_2O_4$
SNL, USA
$CoFe_2O_4$
U. of FL, USA
$CoFe_2O_4$
U. of MN, USA
CeO_2
CNRS, France
SnO_2
PSI/ETH
Switzerland
ZnO

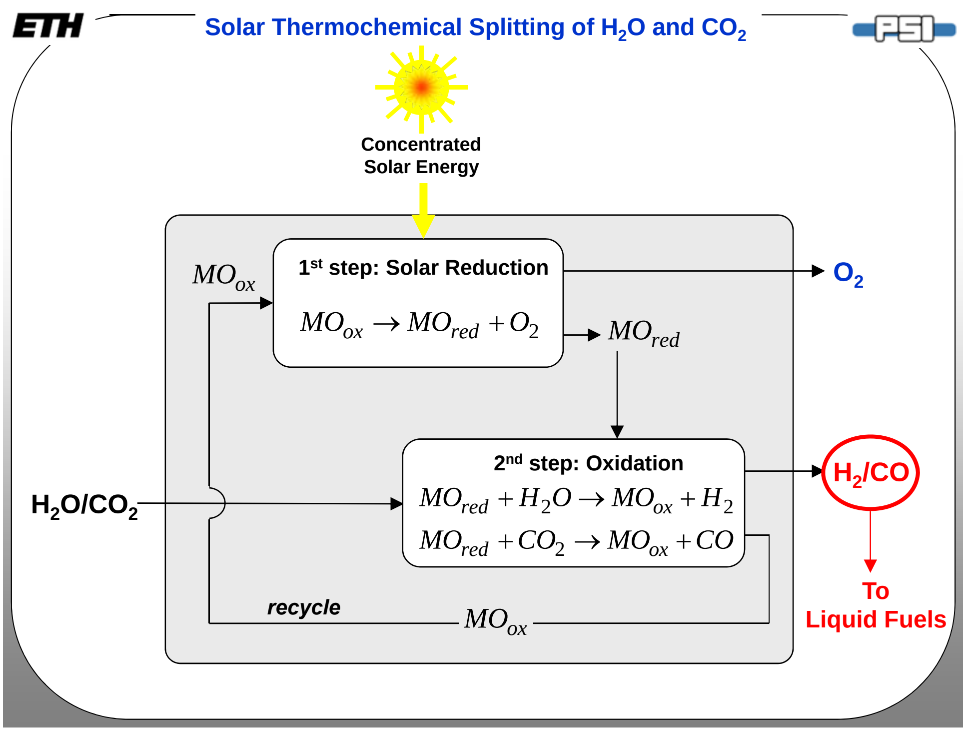
ETH
Solar Thermochemical Splitting of H_2O and CO_2
PSI
Concentrated
Solar Energy
MO_{ox}
1st step: Solar Reduction
$MO_{ox} \rightarrow MO_{red} + O_2$
O_2
MO_{red}
2nd step: Oxidation
$MO_{red} + H_2O \rightarrow MO_{ox} + H_2$
$MO_{red} + CO_2 \rightarrow MO_{ox} + CO$
H_2O/CO_2
H_2/CO
To
Liquid Fuels
recycle
MO_{ox}

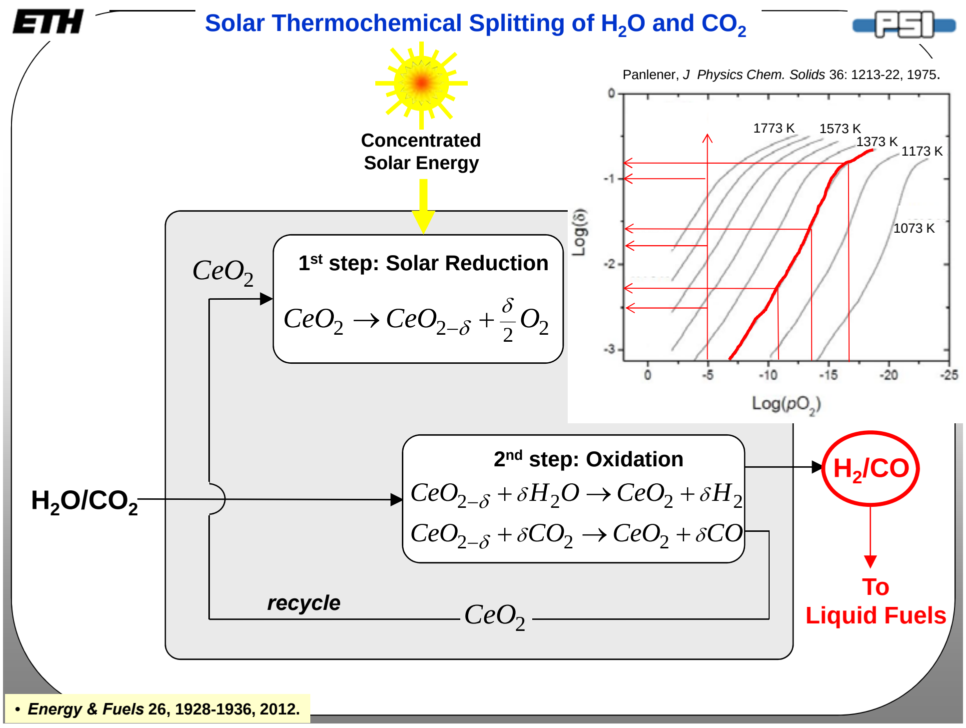
Solar Thermochemical Splitting of H_2O and CO_2
Concentrated Solar Energy
Panlener, J Physics Chem. Solids 36: 1213-22, 1975.
CeO_2
1st step: Solar Reduction
$CeO_2 \rightarrow CeO_{2-\delta} + \frac{\delta}{2} O_2$
1773 K
1573 K
1373 K
1173 K
1073 K
Log(δ)
$\log(pO_2)$
H_2O/CO_2
2nd step: Oxidation
$CeO_{2-\delta} + \delta H_2O \rightarrow CeO_2 + \delta H_2$
$CeO_{2-\delta} + \delta CO_2 \rightarrow CeO_2 + \delta CO$
H_2/CO
To Liquid Fuels
recycle
CeO_2
• Energy & Fuels 26, 1928-1936, 2012.

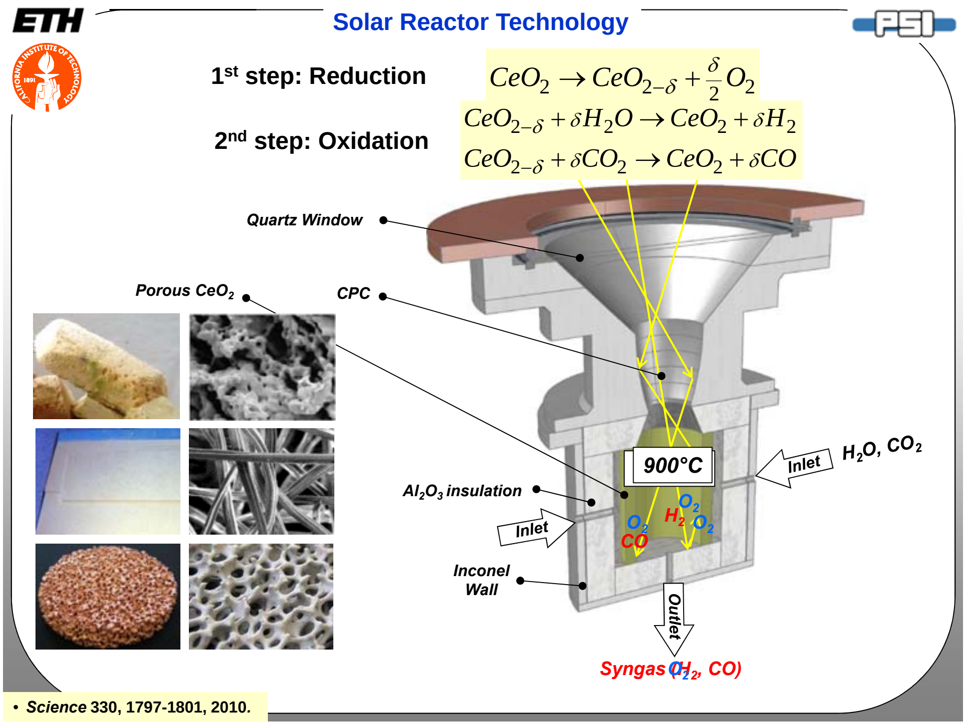
Solar Reactor Technology
1st step: Reduction
$CeO_2 \rightarrow CeO_{2-\delta} + \frac{\delta}{2} O_2$
2nd step: Oxidation
$CeO_{2-\delta} + \delta H_2O \rightarrow CeO_2 + \delta H_2$
$CeO_{2-\delta} + \delta CO_2 \rightarrow CeO_2 + \delta CO$
Quartz Window
Porous CeO_2
CPC
900°C
Inlet
H_2O, CO_2
Al_2O_3 insulation
Inlet
Inconel Wall
Outlet
Syngas (H_2, CO)
• Science 330, 1797-1801, 2010.

Experimental Setup

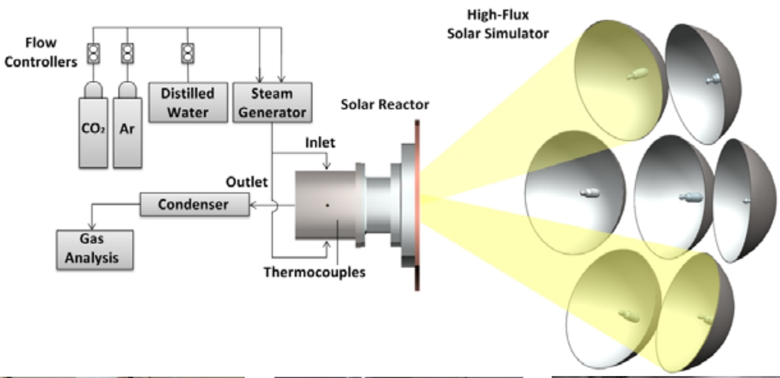

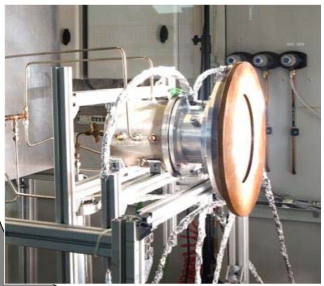

Energy Conversion Efficiency

$$\eta_{\text{solar-to-fuel}} = \frac{[\text{heating value of fuel produced}]}{[\text{solar energy input}] + [\text{energy for inert gas recycling}]}$$

$$\eta_{\text{solar-to-fuel, average}} = \frac{\Delta H \cdot \int r_{\text{fuel}} dt}{\int P_{\text{solar}} dt + E_{inert} \int r_{\text{inert}} dt}$$

$$\eta_{\text{solar-to-fuel, peak}} = \frac{\Delta H \cdot 2 \cdot r_{\text{oxygen}}}{P_{\text{solar}} + E_{inert} r_{\text{inert}}}$$

ΔH_{fuel} = high heating value of the fuel

r_{fuel} = molar fuel production rate

r_{oxygen} = molar O_2 release rate

r_{inert} = flow rate of inert gas

E_{inert} = energy for separation of inert gas from air (20 $kJmol^{-1}$)

P_{solar} = radiative power input

Solar Experimental Results

CeO_2 bricks
- porosity = 76 %
- SSA = 2.7 m^2 g^{-1}

	Reduction	Oxidation
Power Input:	2 kW	1.4 kW
Gas Flow:	2 l min^{-1} Ar	9 l min^{-1} H_2O/CO_2
Ceria Structure:	**Porous monolithic bricks** Total Mass: 325 g	

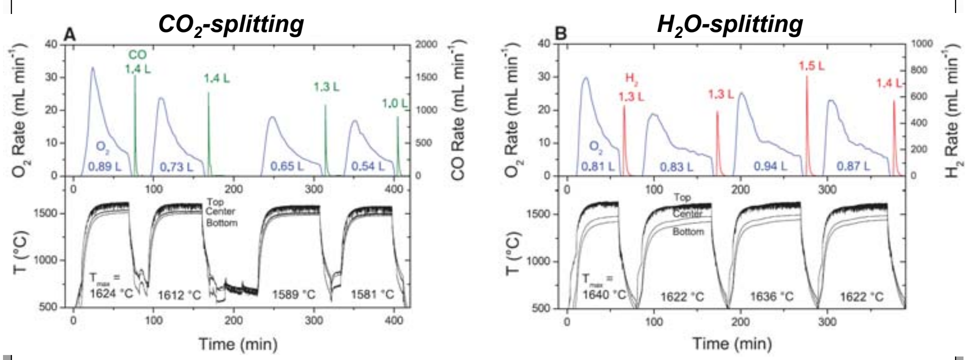

$$\eta_{\text{solar-to-fuel, average}} = 0.4\%$$

$$\eta_{\text{solar-to-fuel, peak}} = \begin{cases} 0.8\% \text{ for } CO_2\text{-splitting} \\ 0.7\% \text{ for } H_2O\text{-splitting} \end{cases}$$

- ***Science*** **330, 1797-1801, 2010.**

Simultaneous H_2O/CO_2-Splitting

CeO_2 felt
- porosity = 96 %
- SSA = 6.0 m^2 g^{-1}

	Reduction	Oxidation
Power Input:	3.6 kW	0.8 kW
Gas Flows:	Ar: 2 l min^{-1}	CO_2: 0.375 l min^{-1} H_2O: 2.15 l min^{-1}
Ceria Structure:	**Felt;** total mass: 127 g	

$H_2O:CO_2$ = 5.7

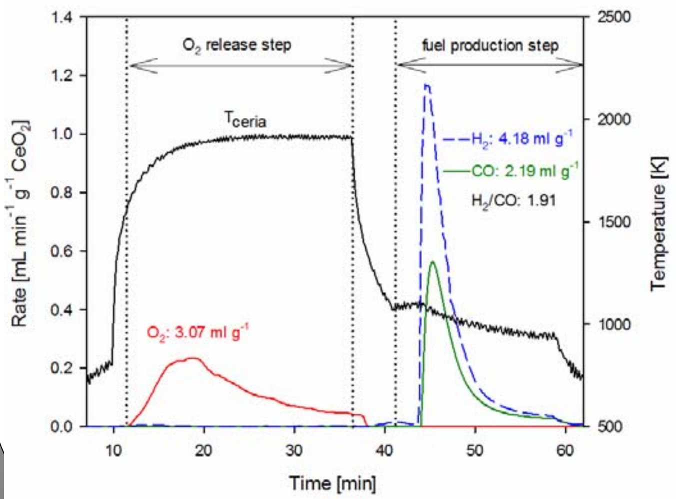

- **O_2 : Fuel = 0.5 ± 0.05**
- **No hydrocarbons**
- **No C depositions**
- **Total selectivity**

- ***Energy & Env. Science*** **5, 6098-6103, 2012.**

Simultaneous H_2O/CO_2-Splitting

CeO_2 felt
- porosity = 96 %
- SSA = 6.0 $m^2 g^{-1}$

	Reduction	Oxidation
Power Input:	3.6 kW	0.7 kW
Gas Flows:	Ar: 2 l min^{-1}	CO_2: 0.33 l min^{-1} H_2O: 2.20 l min^{-1}
Ceria Structure:	Felt , Total Mass: 127 g	

H_2O:CO_2 = 6.7

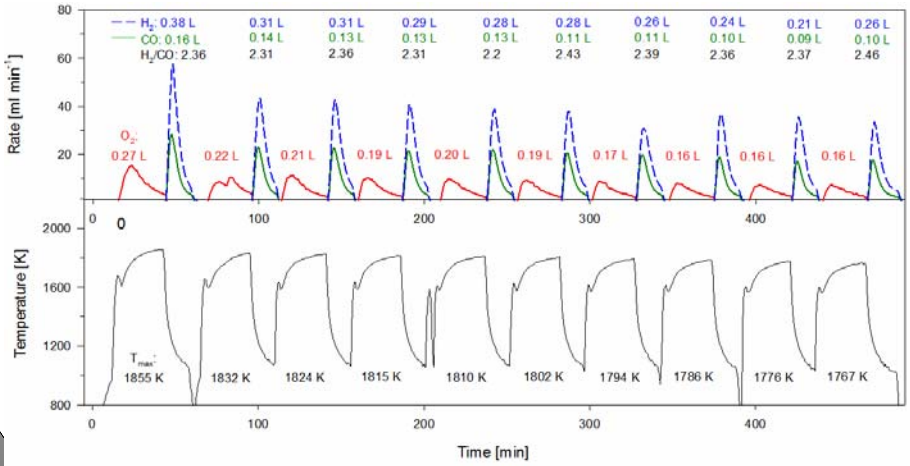

- *Energy & Env. Science* **5, 6098-6103, 2012.**

Simultaneous H_2O/CO_2-Splitting

CeO_2 felt
- porosity = 96 %
- SSA = 6.0 $m^2 g^{-1}$

	Reduction	Oxidation
Power Input:	3.6 kW	0.8 kW
Gas Flows:	Ar: 2 l/min	CO_2: 0.29-1.39 l/min H_2O: 1.11- 2.21 l/min
Ceria structure:	Felt; total mass: 127 g	

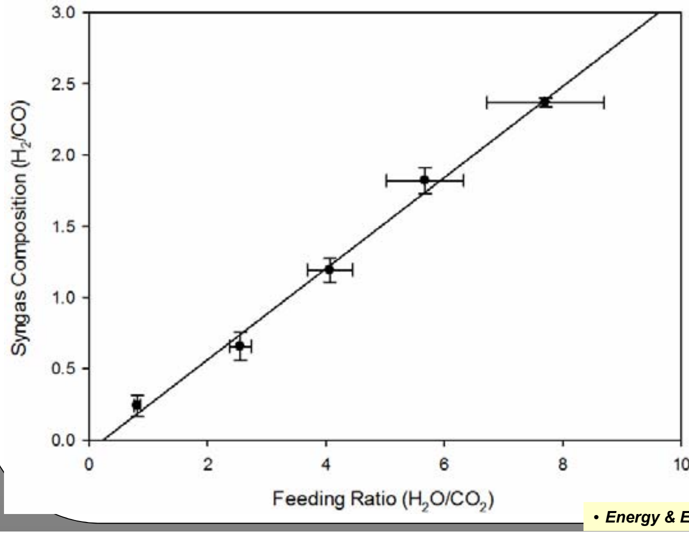

- *Energy & Env. Science* **5, 6098-6103, 2012.**

CO_2-Splitting

ETH EMPA PSI

CeO_2 RPC

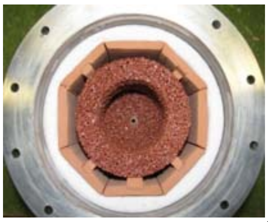

	Reduction	Oxidation
Power Input:	3.8 kW	0 kW
Gas Flow:	2 l min^{-1} Ar	2.5 l min^{-1} CO_2
Ceria Structure:	**RPC**; total mass: 1416 g	

- porosity = 88 %
- SSA = 1.45*10^{-4} m^2/g

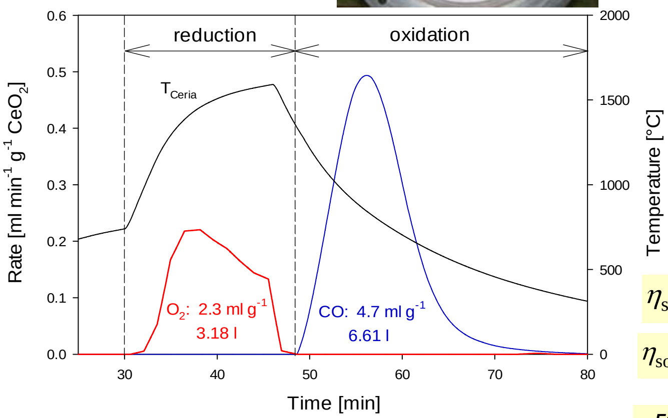

- **O_2 : CO = 0.5 ± 0.1**
- **No hydrocarbons**
- **No C depositions**
- **Total selectivity**

$$\eta_{\text{solar-to-fuel, average}} = 1.73\%$$

$$\eta_{\text{solar-to-fuel, peak}} = 3.53\%$$

- ***Energy & Fuels* 26, 7051–7059, 2012**

CO_2-Splitting

ETH EMPA PSI

CeO_2 felt

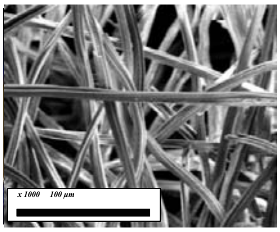

SSA = 6.00 m^2/g

CeO_2 RPC

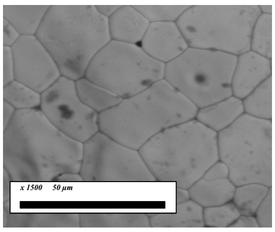

SSA = 1.45*10^{-4} m^2/g

	Reduction	Oxidation
Power Input:	3.6 kW	0.7 kW
Gas Flow:	2 l min^{-1} Ar	3 l min^{-1} CO_2
Ceria Structure:	**RPC** & **Felt**	

Reduction: O_2 evolution

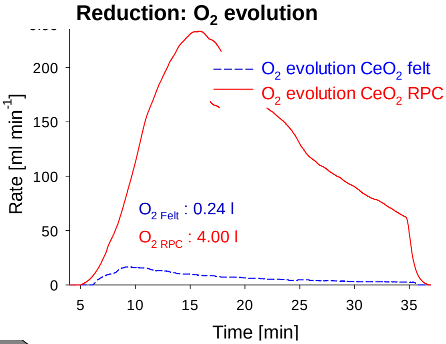

Oxidation: CO evolution

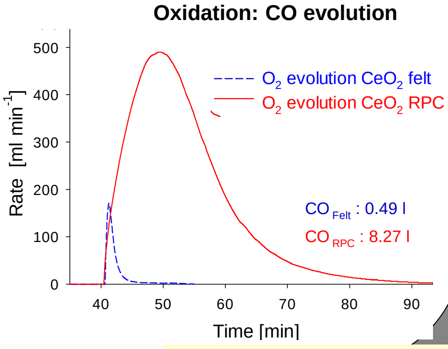

- ***Energy & Fuels* 26, 7051–7059, 2012**

CO_2-Splitting

CeO_2 RPC

	Reduction	Oxidation
Power Input:	3.6 kW	0.7 kW
Gas Flow:	2 l min^{-1} Ar	3 l min^{-1} CO_2
Ceria Structure:	RPC	

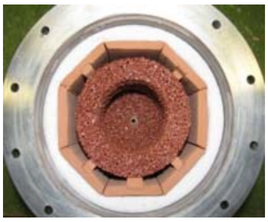

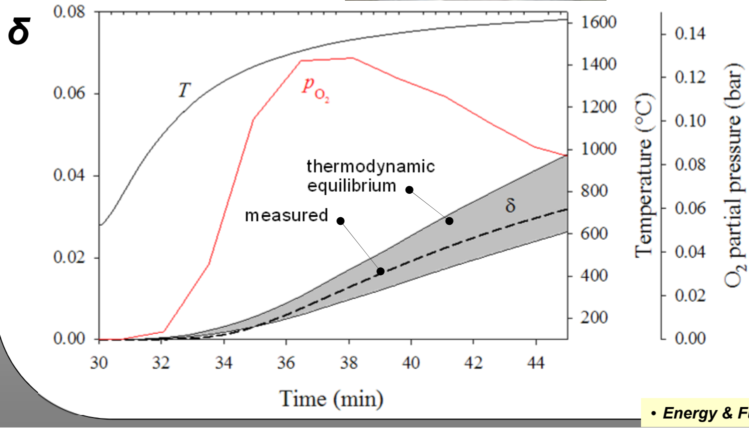

• *Energy & Fuels* 26, 7051–7059, 2012

Reticulate Porous Ceramic (RPC)

- average pore diameter = 2.54 mm
- total porosity = 92%
- specific surface = 11 mm^{-1}

Effective heat/mass transport properties:

- thermal conductivity
- heat transfer coefficient
- permeability
- extinction coefficient
- scattering phase function

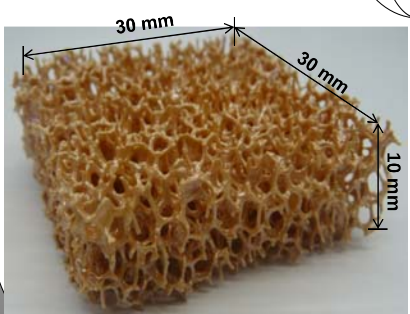

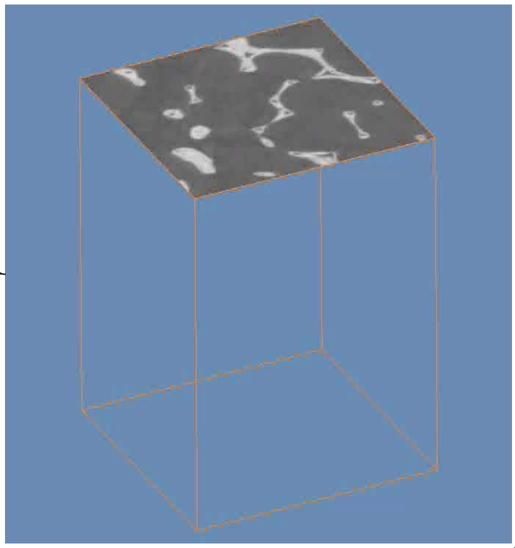

• *J. Heat Transfer* 132, 023305 , 2010.
• *Materials,* 5, 192-209, 2012.

Radiative properties of RPC

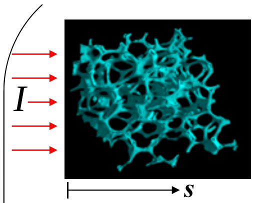

$$\underbrace{\frac{dI_\lambda}{ds}}_{\substack{\text{Change of}\\ \text{radiation}\\ \text{intensity}}} = \underbrace{-\beta_\lambda \cdot I_\lambda}_{\substack{\text{attenuation}\\ \text{by}\\ \text{absorption+scattering}}} + \underbrace{\kappa_\lambda \cdot I_{\lambda b}}_{\substack{\text{augmentation}\\ \text{by}\\ \text{internal emission}}} + \underbrace{\frac{\sigma_{s\lambda}}{4\pi}\int_{\Omega_i=0}^{4\pi} I_\lambda \cdot \Phi \cdot d\Omega_i}_{\substack{\text{augmentation}\\ \text{by}\\ \text{incoming scattering}}}$$

Pore-level radiation

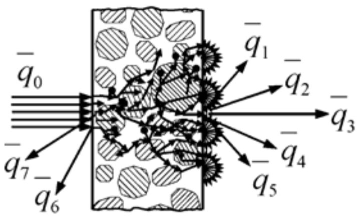

Idealized continuous participating media

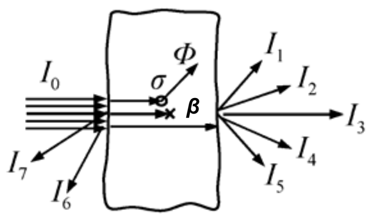

• *ASME J. Heat Transfer* 132, 023305 1-9, 2010.

Radiative properties of RPC

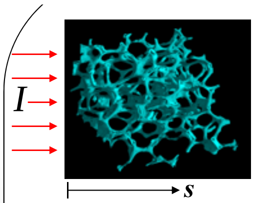

$$\underbrace{\frac{dI_\lambda}{ds}}_{\substack{\text{Change of}\\ \text{radiation}\\ \text{intensity}}} = \underbrace{-\beta_\lambda \cdot I_\lambda}_{\substack{\text{attenuation}\\ \text{by}\\ \text{absorption+scattering}}} + \underbrace{\kappa_\lambda \cdot I_{\lambda b}}_{\substack{\text{augmentation}\\ \text{by}\\ \text{internal emission}}} + \underbrace{\frac{\sigma_{s\lambda}}{4\pi}\int_{\Omega_i=0}^{4\pi} I_\lambda \cdot \Phi \cdot d\Omega_i}_{\substack{\text{augmentation}\\ \text{by}\\ \text{incoming scattering}}}$$

MC ray tracing

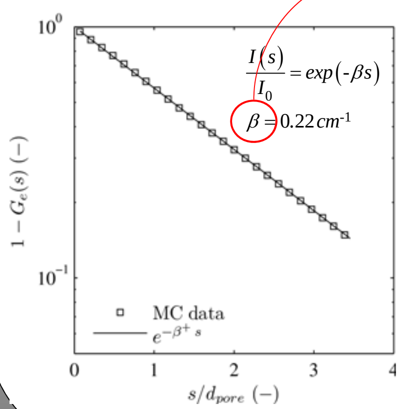

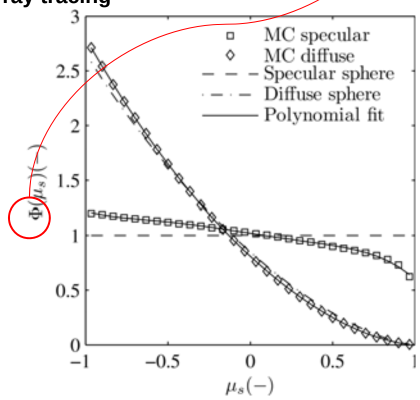

• *ASME J. Heat Transfer* 132, 023305 1-9, 2010.

Fluid transport properties across RPC

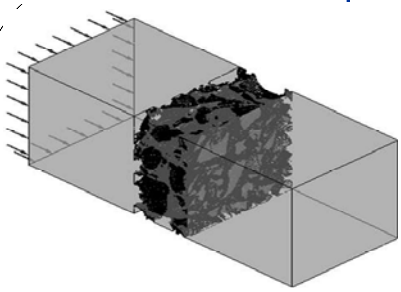

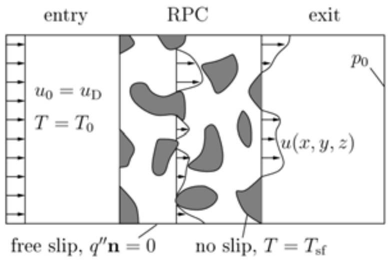

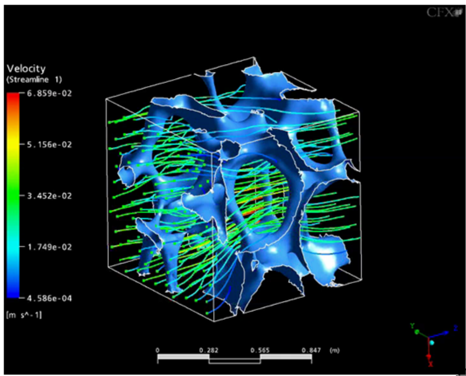

- *Int. J. Heat & Fluid Flow* 29, 315-326, 2008.
- *Materials* 5, 192-209, 2012.

Fluid transport properties across RPC

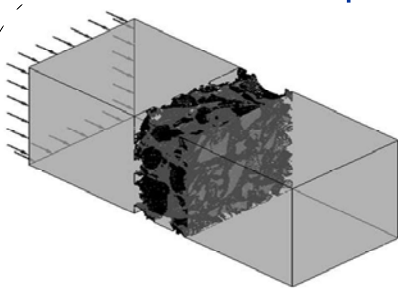

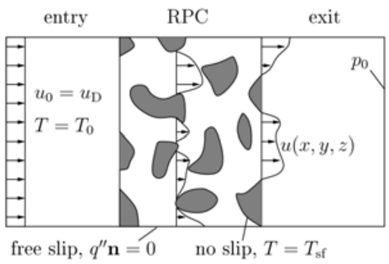

$$\nabla p = -\frac{\mu}{K} u_\mathrm{D} - F \rho \, u_\mathrm{D}^2$$

$$\frac{\nabla p d^2}{\mu \, u_\mathrm{D}} = -c_0 - c_1 \, \mathrm{Re}$$

$$K = 5.69 \cdot 10^{-8} \; m^2$$

$$F = 519.02 \; m^{-1}$$

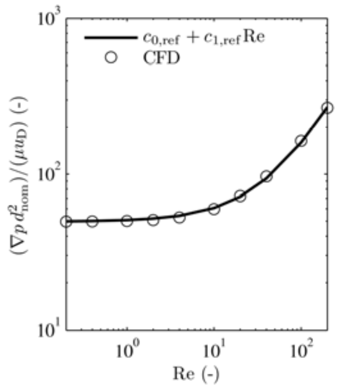

- *Int. J. Heat & Fluid Flow* 29, 315-326, 2008.
- *Materials* 5, 192-209, 2012.

Heat transfer transport across RPC

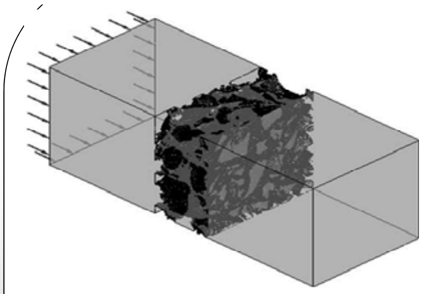

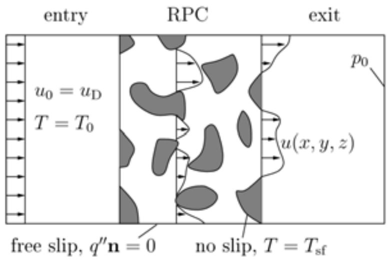

$$h_{sf} = \frac{\int_{z}^{z+\Delta z} q'' \, dA_{sf}}{\Delta T_{lm} \cdot A_{sf}}$$

$$\mathrm{Nu} = 6.82 + 0.19\,\mathrm{Re}^{0.78}\,\mathrm{Pr}^{0.60}$$

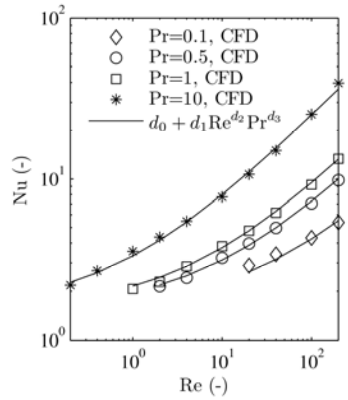

- *Int. J. Heat & Fluid Flow* 29, 315-326, 2008.
- *Materials* 5, 192-209, 2012.

Pore-scale modeling

(*work in progress*)

- conduction
- convection
- radiation
- chemistry

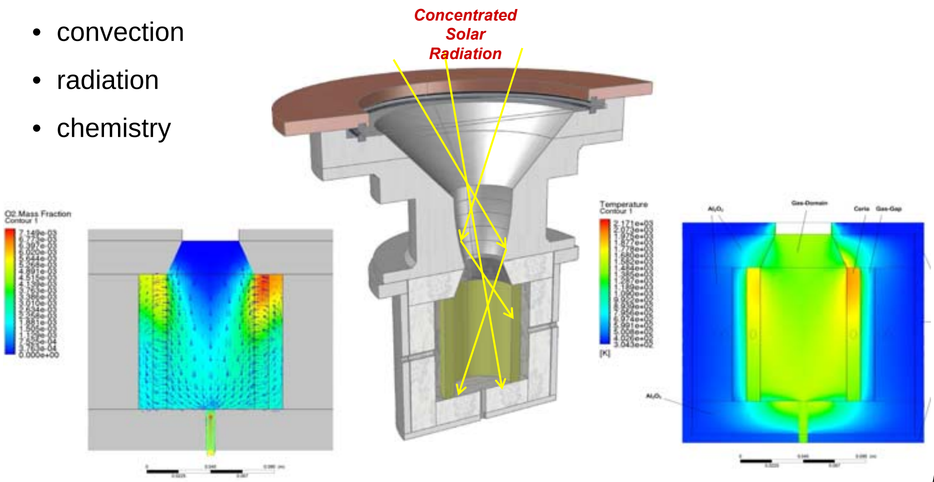

ETH

PSI

Bauhaus Luftfahrt
Neue Wege.

ARTTIC

DLR

SOLAR-JET

Zero-carbon jet fuel from sunlight

ETH

PSI

Source of CO_2 ?

→ **For a true <u>sustainable</u> process, CO_2 should be captured from atmospheric air**

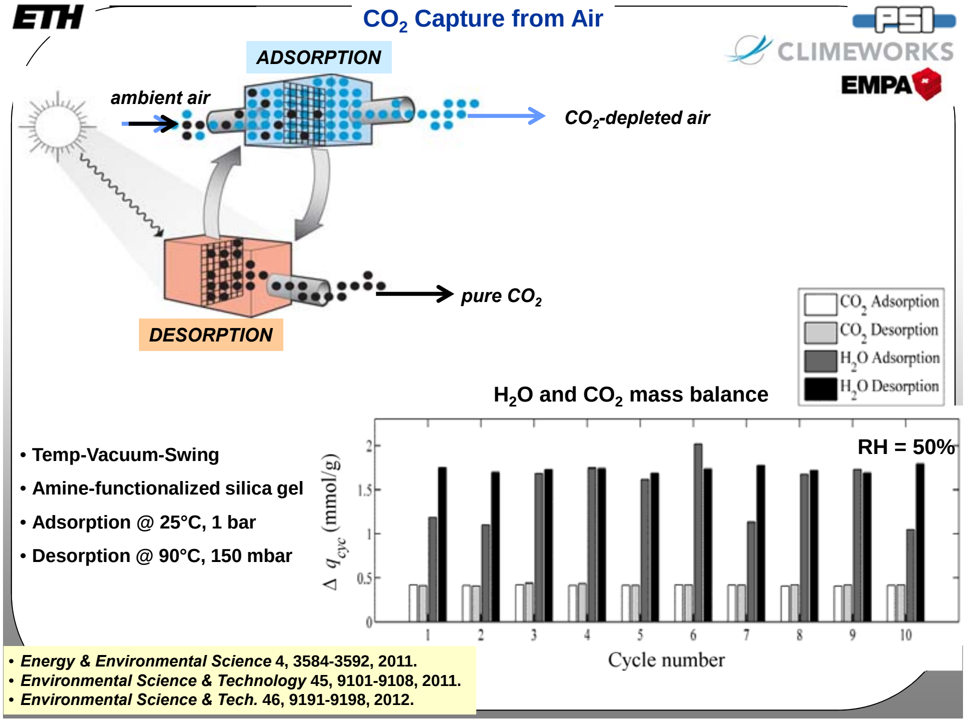
ETH
CO_2 Capture from Air
PSI
CLIMEWORKS
EMPA
ADSORPTION
ambient air
CO_2-depleted air
pure CO_2
DESORPTION
• Temp-Vacuum-Swing
• Amine-functionalized silica gel
• Adsorption @ 25°C, 1 bar
• Desorption @ 90°C, 150 mbar
H_2O and CO_2 mass balance
CO_2 Adsorption
CO_2 Desorption
H_2O Adsorption
H_2O Desorption
RH = 50%
$\Delta\ q_{cyc}$ (mmol/g)
0
0.5
1
1.5
2
1 2 3 4 5 6 7 8 9 10
Cycle number
• *Energy & Environmental Science* 4, 3584-3592, 2011.
• *Environmental Science & Technology* 45, 9101-9108, 2011.
• *Environmental Science & Tech.* 46, 9191-9198, 2012.

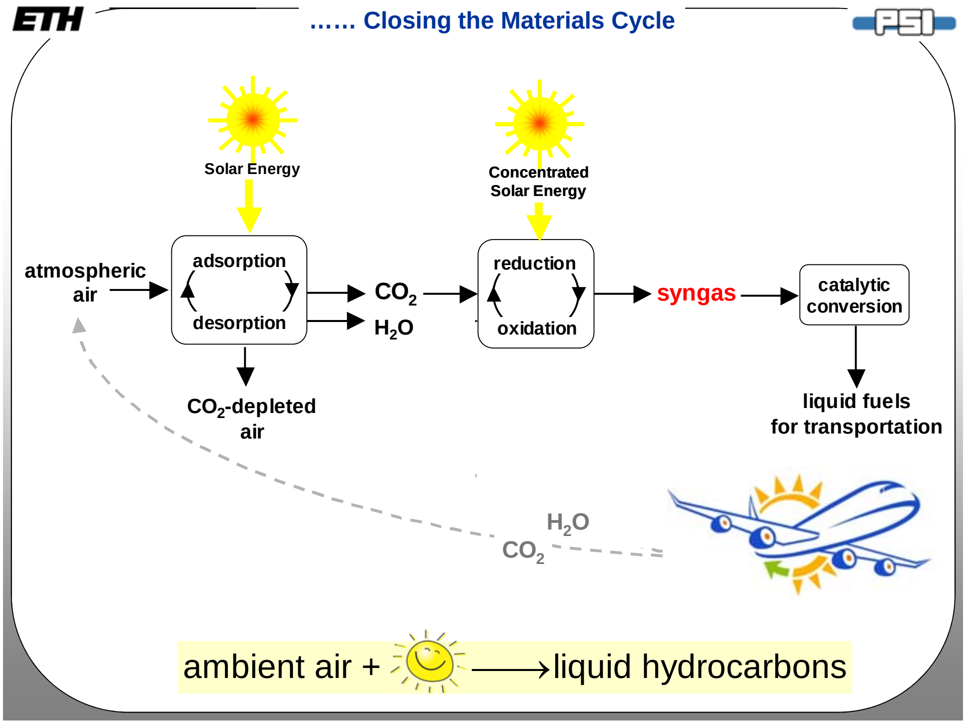
ETH
...... Closing the Materials Cycle
PSI
Solar Energy
Concentrated Solar Energy
atmospheric air
adsorption
desorption
CO_2
H_2O
reduction
oxidation
syngas
catalytic conversion
CO_2-depleted air
liquid fuels for transportation
H_2O
CO_2
ambient air + ⟶ liquid hydrocarbons

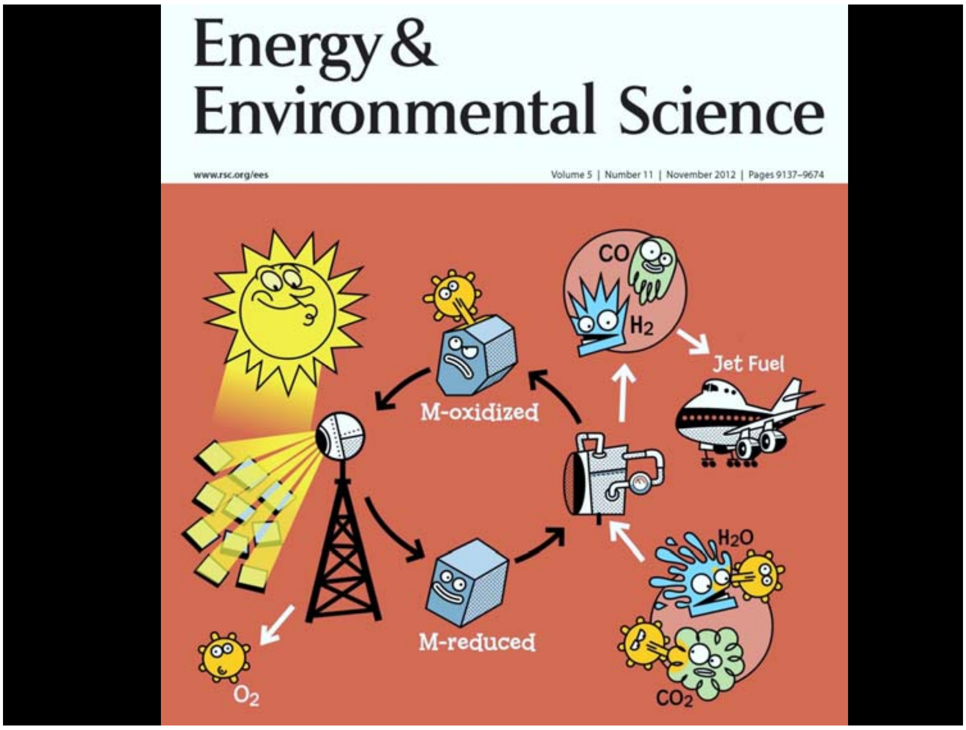
Energy & Environmental Science
www.rsc.org/ees
Volume 5 | Number 11 | November 2012 | Pages 9137–9674
M-oxidized
M-reduced
CO
H_2
Jet Fuel
H_2O
CO_2
O_2